Simon S. Lam, *Packet Switching in a Multi-Access Broadcast Channel with Application to Satellite Communication in a Computer Network*, Ph.D. Dissertation, Computer Science Department, University of California at Los Angeles, March 1974; published as Technical Report UCLA-ENG-7429 (ARPA), School of Engineering and Applied Science, UCLA, April 1974, 306 pages.

Available in eleven .pdf files:

- TRcovers.pdf
- Abstract+ToC.pdf
- Chapter1.pdf
- Chapter2.pdf
- Chapter3.pdf
- Chapter4.pdf
- Chapter5.pdf
- Chapter6.pdf
- Chapters7-8.pdf
- Bibliography.pdf
- Appendices.pdf

CHAPTER 4

CHANNEL DYNAMICS

In the last chapter, analytic models were developed to predict the equilibrium throughput-delay performance of the slotted ALOHA channel under various assumptions. Many of these assumptions (e.g., the independence assumption, the Poisson assumption and the stationarity assumption) represent merely approximations to the physical situation. However, without them the mathematical analysis becomes very complex and solutions are difficult to come by. The source of difficulty lies in the dimensionality of the state vector. (The state vector of a system consists of all the variables of interest such that knowledge of them at time t_1 and knowledge of all system inputs in the interval $[t_1,t_2]$ are sufficient to determine uniquely the state vector at time $t_2 > t_1$.) For the channel model under consideration, we must include in the state vector, channel information for as many time slots as the maximum value of a retransmission delay. Furthermore, each component of the state vector may take on a large number (possibly infinite) of values.

In this chapter, we first formulate a Markov chain model with none of the assumptions mentioned above and obtain a recursive transform equation which characterizes the time behavior of the channel. However, no simple solution to the transform equation has been obtained. Such an exercise in symbol manipulations serves only to illustrate the difficulty and futility of an exact mathematical analysis. Next, we adopt a weakened version of the independence assumption for channel traffic and show, for the infinite population model, that as the uniform randomization interval K approaches infinity, the channel traffic is Poisson distributed. At the same time, the average channel traffic as a function of time is given by a difference equation. This equation permits us to investigate the dynamic behavior of the channel subject to a time varying input. Since only expected values are involved, the difference equation represents a deterministic approximation or fluid approximation [KLEI 74D, NEWE 68] of the original stochastic process. Similar dynamic channel behavior was predicted by Rettberg [RETT 72].

4.1 An Exact Analysis

We shall analyze the slotted ALOHA channel described in Section 2.3 without most of the assumptions made in the last chapter. As before, V^t and X^t are random variables representing the channel input and channel traffic in the t^{th} time slot. The only assumption we shall need in this section is that V^t is an independent process and independent of the channel state. The channel state vector at time t is given by the set of $R + K$ variables $\{X^t, X^{t-1}, \ldots X^{t-R-K+1}\}$. (Note that $R + K$ is the maximum value of a retransmission delay.) We define the channel state vector

$$\underline{X}^t = \begin{bmatrix} X_1^{\ t} \\ X_2^{\ t} \\ \vdots \\ X_{R+K}^{\ t} \end{bmatrix} = \begin{bmatrix} X^t \\ X^{t-1} \\ \vdots \\ X^{t-R-K+1} \end{bmatrix}$$

which is a random vector with probability distribution

$$P^t(\underline{x}) = \text{Prob}\ [\underline{X}^t = \underline{x}] \qquad \underline{x} \in S$$

where S is the admissible state space and $\underline{x}$ is an integer-valued $(R + K)$-dimensional vector in S. $\underline{X}^t$ is a discrete state discrete time Markov chain which will be completely specified by its one-step state transition probabilities

$$P^t(\underline{y}|\underline{x}) = \text{Prob}[\underline{X}^{t+1} = \underline{y}|\underline{X}^t = \underline{x}] \qquad \underline{x},\underline{y} \in S$$

such that

$$P^{t+1}(\underline{y}) = \sum_{\underline{x}\in S} P^t(\underline{y}|\underline{x})P^t(\underline{x}) \qquad \underline{y} \in S \tag{4.1}$$

We now define,

$$v_i^{\,t} = \text{Prob}[V^t = i] \qquad i = 0, 1, 2, \ldots$$

and

$$\lambda(m) = \begin{cases} 0 & m = 1 \\ m & m \neq 1 \end{cases}$$

The one-step state transition probabilities at time t for the Markov chain $\underline{X}^t$ are given below.

$$P^t(\underline{y}|\underline{x}) = \begin{cases} 0 & \text{if } y_i \neq x_{i-1} \\ & \forall\ i = 2, 3, \ldots, R{+}K \\ \displaystyle\sum_{\substack{i=0 \\ i\leq \ell}}^{y_1} v^{t+1}_{y_1-i} \binom{\ell}{i} \left(\frac{1}{K}\right)^i \left(1-\frac{1}{K}\right)^{\ell-i} & \text{otherwise} \end{cases} \tag{4.2}$$

where

$$\ell = \sum_{j=1}^{K} \lambda(x_{R+j})$$

is the total number of packets which collided in the K slots (from the $(t - R)^{th}$ to the $(t - R - K + 1)^{th}$) such as shown in Fig. 3.1. Note that each such packet retransmits into the $(t + 1)^{st}$ slot independently with probability $\frac{1}{K}$. Note also that for $i = 2, 3, \ldots, R + K$, the event $[y_i \neq x_{i-1}]$ is impossible and thus has zero probability (since both y_i and x_{i-1} represent the value of channel traffic in the same time slot).

Now given an initial probability distribution for the channel traffic in $R + K$ consecutive time slots, the stochastic behavior of the channel as a function of time is predicted by Eqs. (4.1) and (4.2).

<u>A recursive transform equation</u>

We first define the following transforms,

$$V^t(z) = \sum_{i=0}^{\infty} z^i \, v_i^{\,t}$$

and

$$Q^t(\underline{z}) = Q^t(z_1, z_2, \ldots, z_{R+K})$$

$$= \sum_{x_1=0}^{\infty} \cdots \sum_{x_{R+K}=0}^{\infty} \left(\prod_{j=1}^{R+K} z_j^{\,x_j} \right) p^t(\underline{x})$$

From Eqs. (4.1) and (4.2), a recursive transform equation relating $Q^{t+1}(\underline{z})$ to $V^{t+1}(z)$ and $Q^t(\underline{z})$ can be derived (see Appendix C) and is given below.

$$Q^{t+1}(\underline{z}) = V^{t+1}(z_1)\left[\sum_{\{(\varepsilon_1,\ldots,\varepsilon_K)\,|\,\varepsilon_j=0,1\}} Q^t(\underline{z};\underline{\varepsilon})\right] \tag{4.3}$$

where $\underline{\varepsilon}$ is a K-dimensional vector and $Q^t(\underline{z};\underline{\varepsilon})$ for a given $\underline{\varepsilon}$ can be obtained from $Q^t(\underline{z})$ by the following algorithm:

(1) Initialize $Q^t(\underline{z};\underline{\varepsilon}) \leftarrow Q^t(z_2,\ldots,z_{R+1},y_1,\ldots,y_K)$ and $j \leftarrow 1$

(2) If $j = K$, go to (5)

(3) If $\varepsilon_j = 0$,

replace y_j by $z_{R+j+1}\left(1 - \frac{1}{K} + \frac{z_1}{K}\right)$ in $Q^t(\underline{z};\underline{\varepsilon})$,

else $Q^t(\underline{z};\underline{\varepsilon}) \leftarrow z_{R+j+1}\,\frac{(1-z_1)}{K} \cdot \frac{\partial}{\partial y_j} Q^t(\underline{z};\underline{\varepsilon})\Big|_{y_j = 0}$

(4) $j \leftarrow j + 1$ and go to (2)

(5) If $\varepsilon_K = 0$,

replace y_K by $\left(1 - \frac{1}{K} + \frac{z_1}{K}\right)$ in $Q^t(\underline{z};\underline{\varepsilon})$,

else $Q^t(\underline{z};\underline{\varepsilon}) \leftarrow \frac{1-z_1}{K} \cdot \frac{\partial}{\partial y_K} Q^t(\underline{z};\underline{\varepsilon})\Big|_{y_K = 0}$

The notation $A \leftarrow F(A)$ means: evaluate $F(A)$ which then becomes the new expression for A. As an example, for the case when $R = 2$ and $K = 2$, we get the following transform equation.

$$Q^{t+1}(z_1,z_2,z_3,z_4) = V^{t+1}(z_1)\Bigg[Q^t\left(z_2,z_3,z_4\left(1-\frac{1}{K}+\frac{z_1}{K}\right),\left(1-\frac{1}{K}+\frac{z_1}{K}\right)\right)$$

$$+\frac{z_4(1-z_1)}{K}\cdot\frac{\partial}{\partial y_1}Q^t\left(z_2,z_3,y_1,\left(1-\frac{1}{K}+\frac{z_1}{K}\right)\right)\Bigg|_{y_1=0}$$

$$+\frac{1-z_1}{K}\cdot\frac{\partial}{\partial y_2}Q^t\left(z_2,z_3,z_4\left(1-\frac{1}{K}+\frac{z_1}{K}\right),y_2\right)\Bigg|_{y_2=0}$$

$$+\frac{z_4(1-z_1)^2}{K^2}\frac{\partial^2}{\partial y_1\partial y_2}Q^t(z_2,z_3,y_1,y_2)\Bigg|_{y_1,y_2=0}\Bigg]$$

The above equation demonstrates the complexity of the transform equation even for small values of R and K. No solution to Eq. (4.3) has been found. The above analysis serves to illustrate the difficulty and futility of an exact mathematical analysis and motivates our use of approximations.

4.2 An Approximate Solution

In this section, we shall analyze the same model above with an additional assumption. We shall assume that the channel traffic within any K consecutive time slots are independent of each other* so that it suffices to solve for the probabilities,

$$P_i^{\,t} = \text{Prob}[X^t = i] \qquad\qquad i = 0, 1, 2, \ldots$$

and the transform,

$$Q^t(z) = \sum_{i=0}^{\infty} z^i P_i^{\,t}$$

*This is a weakened version of the independence assumption for channel traffic used in Chapter 3 and will be referred to as the weak independence assumption for channel traffic. Recall that the (strong) independence assumption gave very accurate results as verified by simulations in Chapter 3.

instead of $Q^t(\underline{z})$. We define the expected values of the random variables X^t and V^t as

$$G^t = E[X^t]$$

and

$$S^t = E[V^t]$$

<u>Another transform equation</u>

A transform equation similar to Eq. (4.3) can be derived under the weak independence assumption (see Appendix C) and is given below.

$$Q^t(z) = V^t(z) \prod_{j=1}^{K} \left[Q^{t-R-j}\left(1 - \frac{1}{K} + \frac{z}{K}\right) + P_1^{\,t-R-j} \; \frac{1-z}{K} \right] \qquad (4.4)$$

Eq. (4.4) can be solved recursively for $Q^t(z)$ given initial probability distributions of the channel traffic in $R + K$ consecutive time slots. Alternatively, $Q^t(z)$ can be approximated arbitrarily well by solving for $P_1^{\,t}$ and a finite number of the moments of the channel traffic X^t . (Note that $P_1^{\,t}$ represents the expected channel throughput in the t^{th} time slot.) By differentiating Eq. (4.4) with respect to z and setting z equal to zero, we obtained the following difference equation for G^t under our assumptions.

$$G^t = \frac{1}{K} \sum_{j=1}^{K} \left[G^{t-R-j} - P_1^{\,t-R-j} \right] + S^t \qquad (4.5)$$

Theorem 4.1 If the channel input is an independent Poisson process, then the channel traffic is Poisson distributed in the limit as $K \to \infty$ under the weak independence assumption, such that

$$Q^t(z) = e^{-G^t(1-z)} \tag{4.6}$$

and

$$P_1{}^t = G^t e^{-G^t} \tag{4.7}$$

where

$$G^t = \frac{1}{K} \sum_{j=1}^{K} \left(G^{t-R-j} - G^{t-R-j} e^{-G^{t-R-j}} \right) + S^t \tag{4.8}$$

Proof See Appendix C.

Equation (4.8) characterizes (approximately) the time behavior of the channel traffic subject to a time varying input when K is large. However, since only expected values are considered, this equation represents a fluid approximation of the stochastic process X^t. To incorporate statistical effects into the time behavior of the system, other techniques which account for some of the higher moments of X^t such as diffusion approximation [KLEI 74D, NEWE 68] may be employed.

Channel saturation described in the last chapter may arise as a result of either (a) statistical fluctuaions, or (b) time variations in the channel input. The effect of statistical fluctations will be studied in the next chapter. The effect of time varying inputs is examined below using Eq. (4.8).

4.3 Some Fluid Approximation Results

Given the Poisson channel input rate as a function of time, the expected channel traffic as a function of time can be obtained from the fluid approximation given by Eq. (4.8). In Figs. 4-1 and 4-2, we show the channel response to two input pulses. In both cases the channel input rate is initially equal to 0.3 packet/slot with the channel in equilibrium. The input rate is then increased to 0.8 packet/slot (well above the channel capacity of 0.368 packet/slot for an infinite population model) for 100 time slots. As a result, the channel traffic rate increases rapidly as the channel throughput rate decreases. The expected channel backlog (defined to be the net area between the channel input and throughput curves and corresponds to the expected total number of packets awaiting retransmission in all channel users) builds up. At the end of the 100 time slots, the channel input rate is reduced to 0.15 packet/slot in the first case. We see that the channel slowly returns to an equilibrium state (see Fig. 4-1). In the second case, the channel input rate is reduced at the end of the pulse to 0.25 packet/slot which, as we see in Fig. 4-2, is not small enough to prevent the channel from saturation. Simulations were performed for both cases using the simulation program developed for the infinite population model. The results are shown in Figs. 4-3 and 4-4. Note that each simulation point indicated actually represents an average value over a period of 50 time slots. Four simulations are shown for each of the two cases. We see that the fluid approximation results in Figs. 4-1 and 4-2 predict the

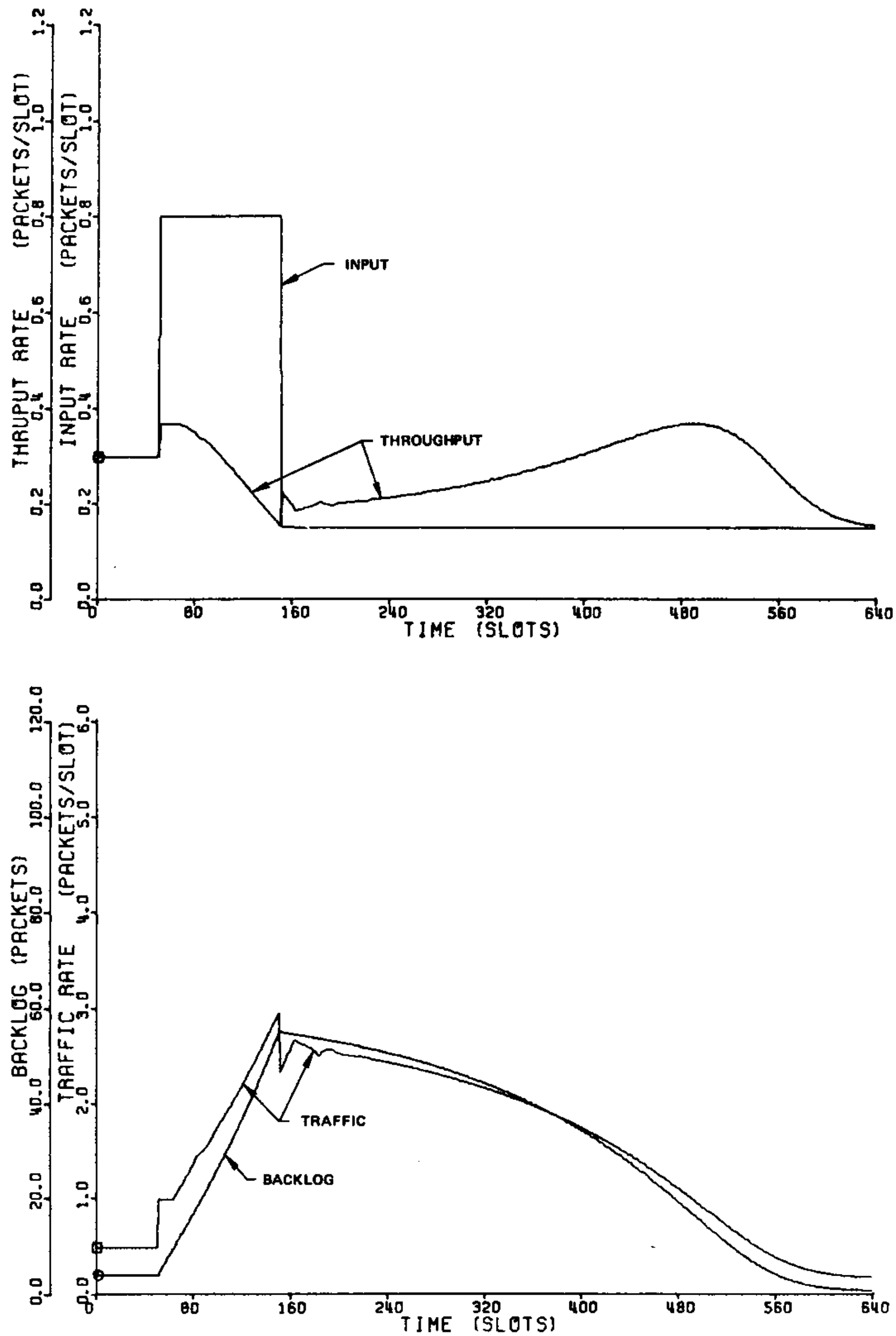

Figure 4-1. Channel Response to an Input Pulse (R = 12, K = 20).

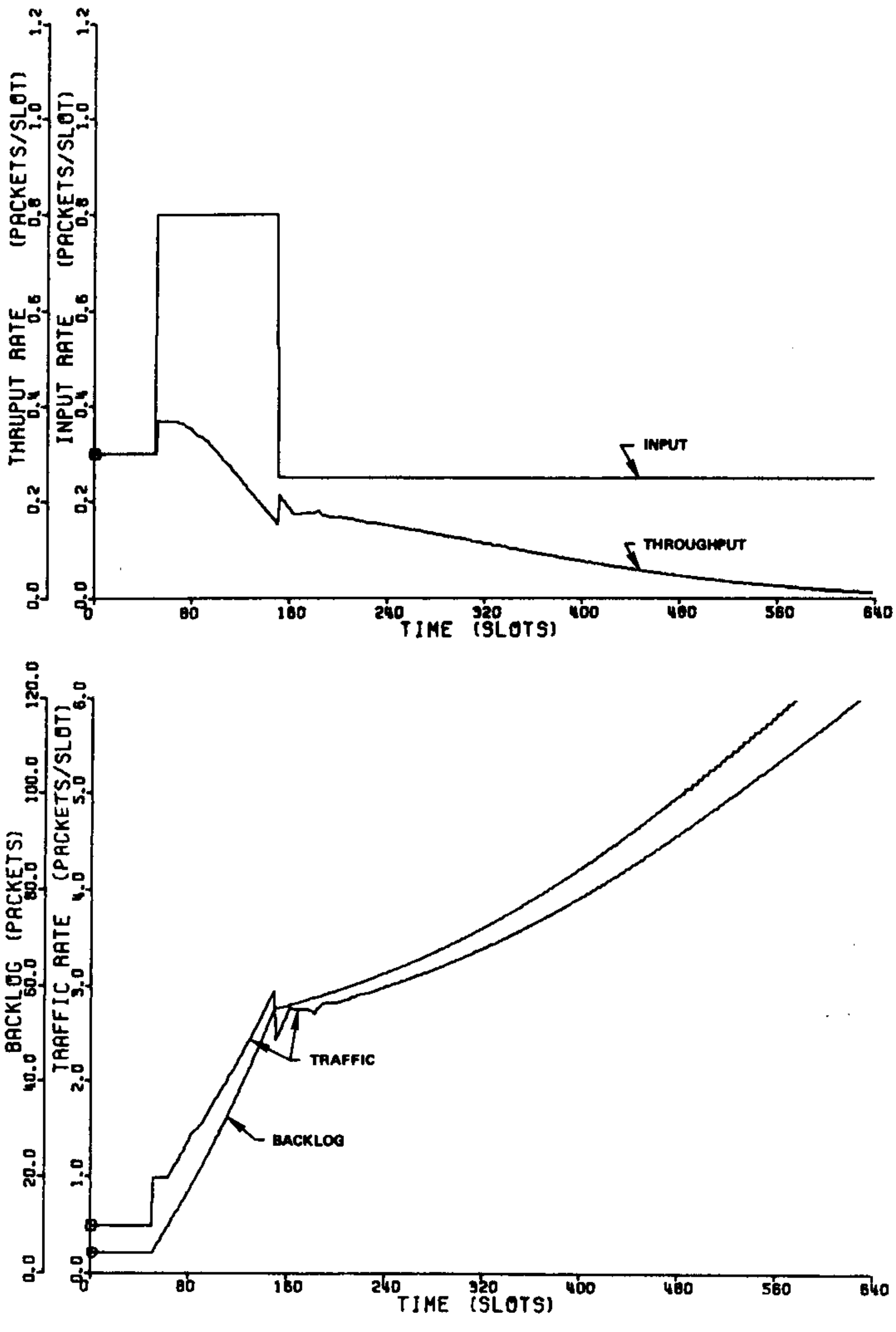

Figure 4-2. Channel Saturation (R = 12, K = 20)

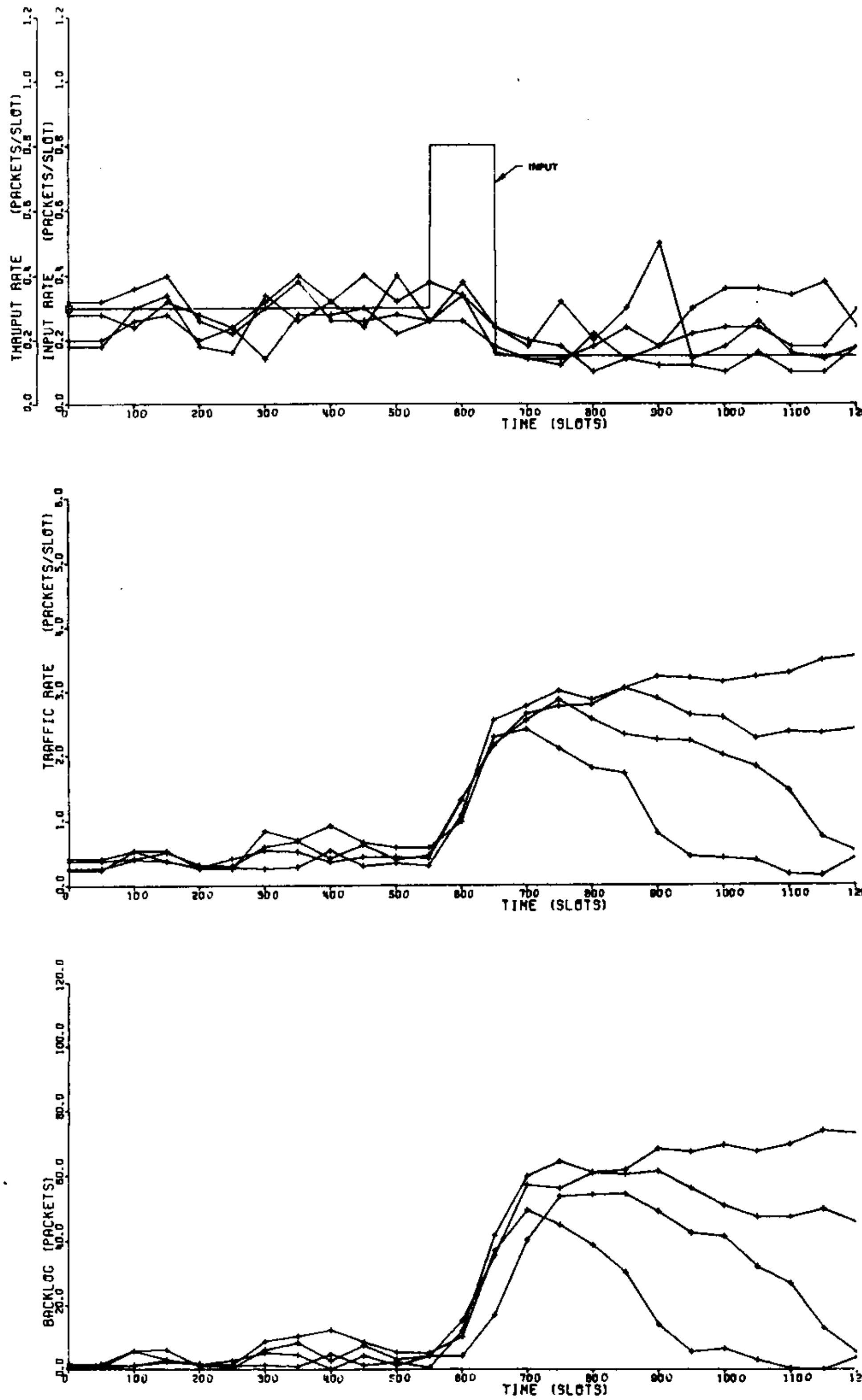

Figure 4-3. Simulations Corresponding to Figure 4-1.

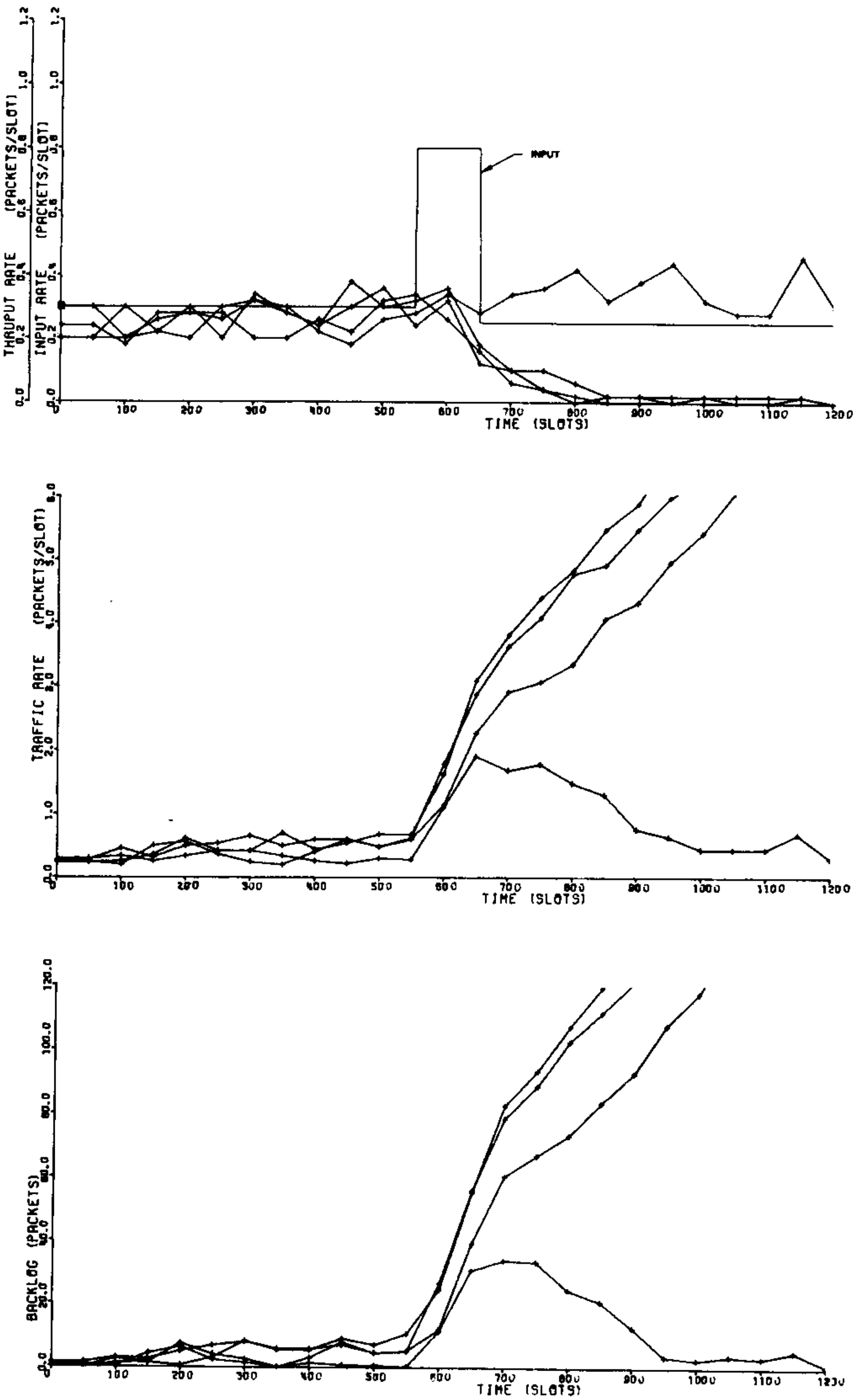

Figure 4-4. Simulations Corresponding to Figure 4-2.

general trend of the simulations. However, since the fluid approximation does not account for statistical fluctuations, there exist large variations among the simulation results.

In Fig. 4-5, we show, using Eq. (4.8), the channel response to a ramp pulse ("impulse") in the channel input rate. At the end of the pulse, the channel input rate is reduced to a small enough value so that the channel is able to return to an equilibrium state. Note that the channel has a natural frequency equal to the inverse of the expected retransmission delay (which is $R + (K + 1)/2$). (In Figs. 4-1 and 4-2 the channel oscillations are less pronounced as a result of a smaller input pulse and a larger K.)

In Fig. 4-6, we present results from the following experiment using Eq. (4.8). Starting with an equilibrium channel, an input pulse is applied until the expected channel backlog reaches some specified value B. The channel input rate is then reduced to some fixed value S'. The time the channel takes to return to an equilibrium state (the recovery time) is measured. (The criterion we adopt here for channel equilibrium is that the channel traffic rate must be less than one for $R + K$ consecutive time slots.) The experiment was carried out numerically using Eq. (4.8) for both rectangular and ramp pulses with different amplitudes. The initial equilibrium channel input rate $S_e = 0.2$ or 0.3 packet/slot. The channel recovery

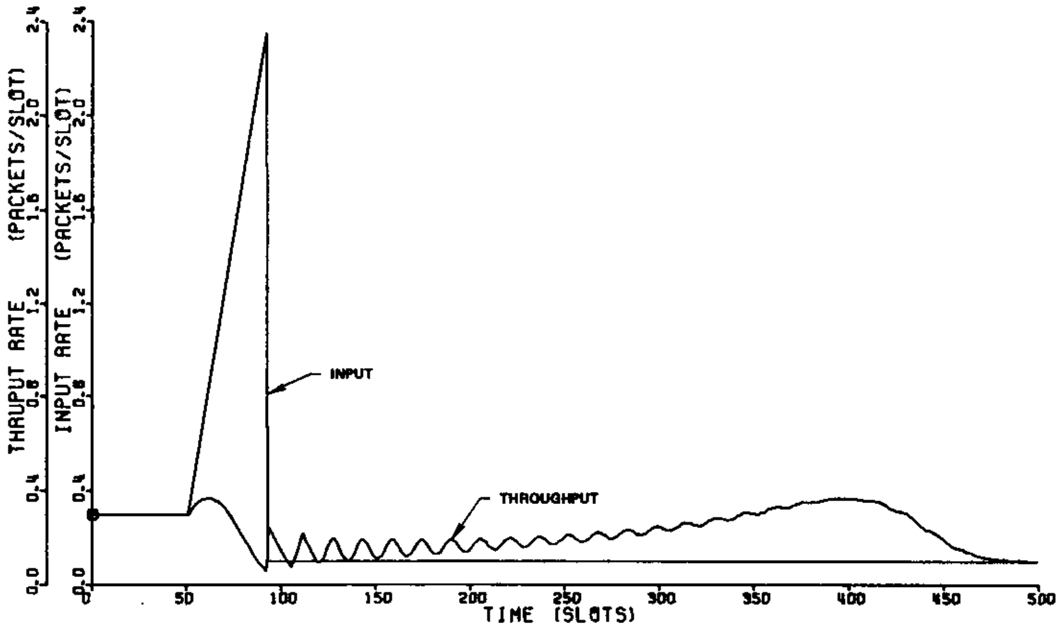

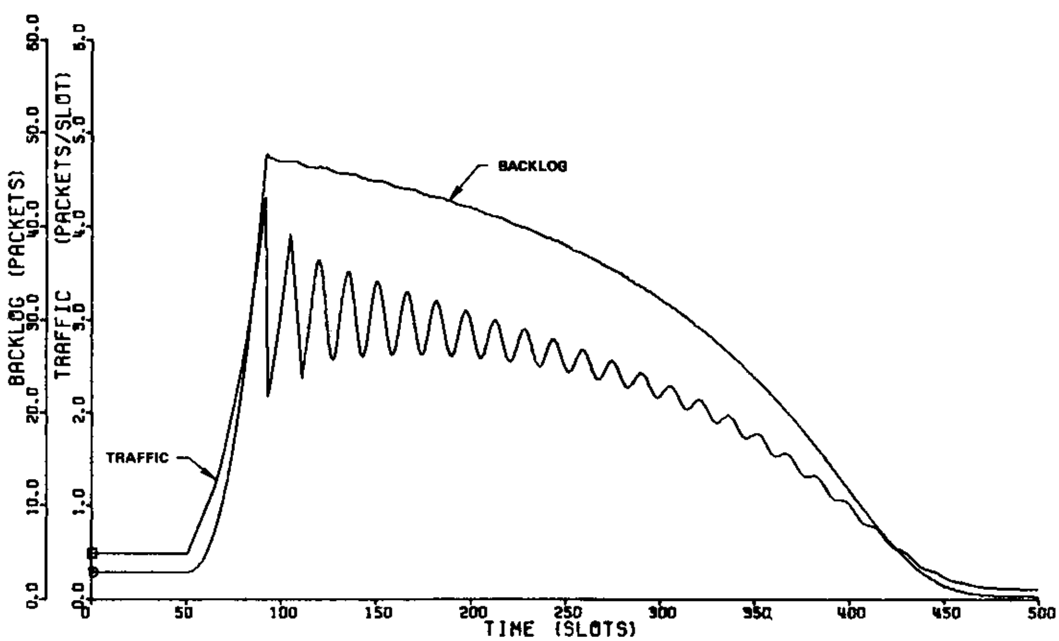

Figure 4-5. Channel Response to a Ramp Pulse (R = 12, K = 6).

time for the cases* considered is shown in Fig. 4-6 as a function of B for constant values of S'. Note that given S' there is a maximum value of B above which the channel recovery time is infinite, in which case a smaller S' must be used. It is interesting to note that the channel recovery time is insensitive to both the shape of the input pulse and S_e. The relevant variables are just B and S'. Recall that the expected channel backlog is the net area between the input and throughput curves. Thus, our results seem to indicate that the channel impulse response depends only upon the area under the impulse but not its shape, which reminds us of the response of linear systems [SCHW 65]! These results also suggest that instead of defining a complex state description such as in the previous sections, the channel behavior may be characterized quite adequately using the channel backlog size alone as a state variable.

---

*Four cases are considered:

(1) rectangular pulse, peak value = 2.35, $S_e = 0.3$

(2) rectangular pulse, peak value = 2.35, $S_e = 0.2$

(3) rectangular pulse, peak value = 1.35, $S_e = 0.3$

(4) ramp pulse, $S(t) = 0.35 + 0.05t$, $S_e = 0.3$

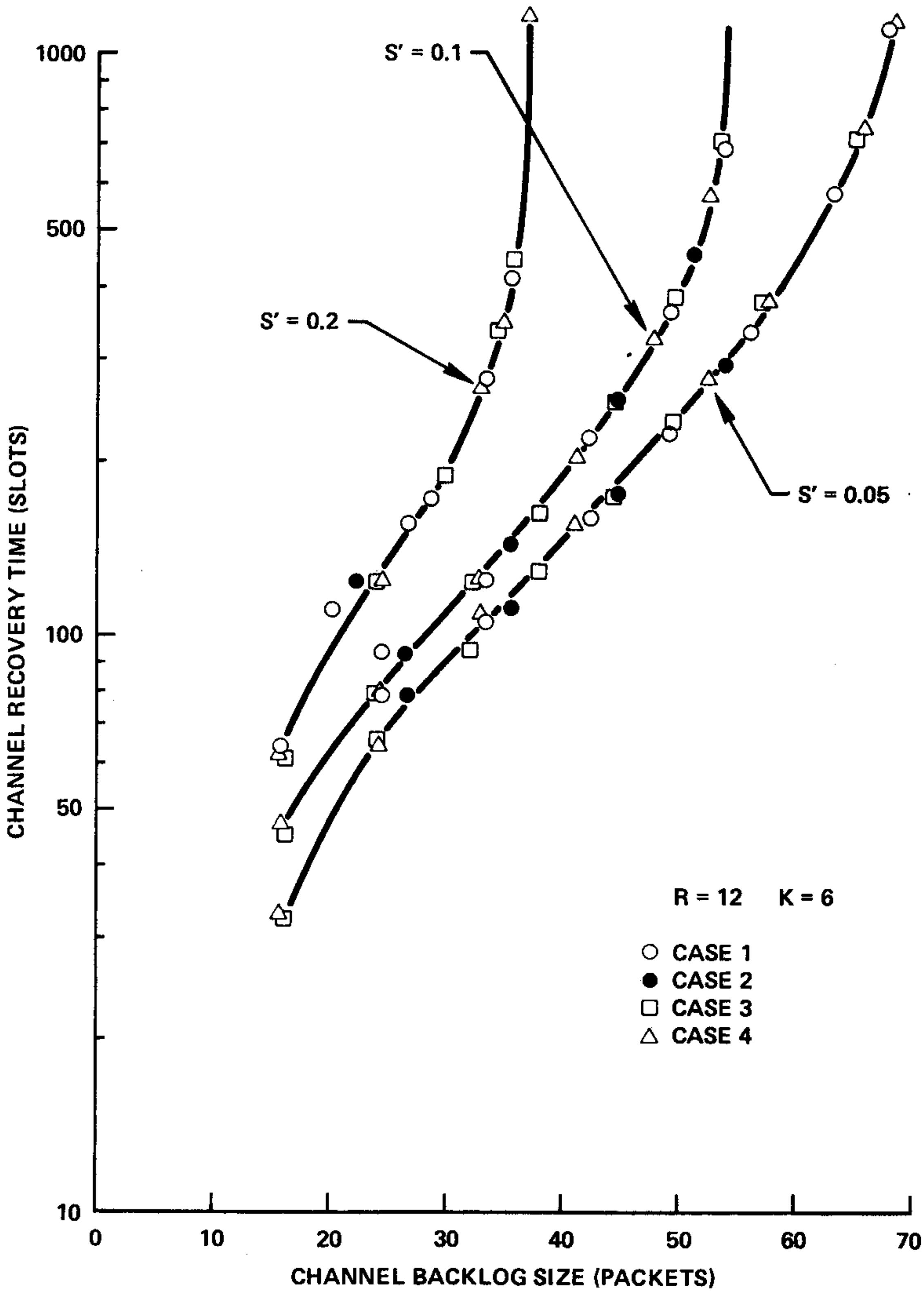

Figure 4-6. Channel Recovery Time Versus Channel Backlog Size (R = 12, K = 6)